DOI 10.5162/Ultrasonic2025/A5-a1

Acoustic Wave Propagation in Porous Piezoelectric Media

Zhixiang Sun[1,2], *Yinqiu Zhou*[1,2], *Xiuming Wang*[1,2], *Lin Liu*[1,2], *Xiao He*[1,2], *and Yonghao Lu*[1,2]
[1]*Institute of Acoustics, Chinese Academy of Sciences, Beijing 100190, China*
[2]*University of Chinese Academy of Sciences, Beijing 100049, China*
zhouyinqiu@mail.ioa.ac.cn

Abstract: Porous piezoelectric media are heterogeneous complex materials composed of a piezoelectric solid skeleton with fluid-filled pores, holding significant value in transducer optimization and understanding bone regeneration mechanisms. However, existing studies are predominantly theoretical, lacking rigorous full-wavefield numerical simulations, particularly accurate treatment of the coupled poroelastic and piezoelectric effects. To address this issue, this work develops a high-fidelity staggered-grid finite-difference time-domain (FDTD) framework for simulating acoustic wave propagation in anisotropic porous piezoelectric media. A mechanical-electrical coupled staggered grid rigorously handles electromechanical coupling by solving Poisson's equation at each time step. Numerical results are validated against analytical solutions from the Christoffel equation, demonstrating superior accuracy compared to simplified coupling schemes.

Keywords: Porous piezoelectric media, FDTD, Biot theory, Poisson's equation, Staggered grid

Introduction

Porous piezoelectric media (PPMs) consist of a piezoelectric solid skeleton with fluid-filled pores, such as porous piezoelectric ceramics and human bone tissue. Compared to traditional dense piezoelectric materials, PPMs exhibit advantages including low density, low acoustic impedance, and low mechanical quality factor, making them valuable for optimizing the acoustic performance of porous piezoelectric composites and transducers, as well as understanding the regeneration mechanisms of piezoelectric bone tissue [1].

Currently, theoretical research on PPMs is primarily based on classical Biot theory [2, 3]. Vashishth and Gupta combined Biot theory with piezoelectric effects, deriving the Christoffel equation for transversely isotropic PPMs [4]; Sharma investigated the effects of piezoelectricity on wave velocities [5]. Regarding numerical simulations, methods have been developed for non-porous piezoelectric materials [6, 7] and non-piezoelectric porous media [8], but rigorous full-wavefield simulations for PPMs remain scarce. Meanwhile, under quasi-static approximation, some numerical studies have employed oversimplified electromechanical coupling treatments, which actually introduce artificial stiffening effects and break the intrinsic anisotropic symmetry of the material [9, 10].

To address these issues, this work proposes a mechanical-electrical coupled staggered-grid FDTD framework for simulating wave propagation in porous piezoelectric media. The method rigorously couples mechanical and electrical fields by solving Poisson's equation at each time step, ensuring numerical stability and physical accuracy. We validate numerical results against analytical solutions based on the Christoffel equation, demonstrating that the rigorous Poisson-based coupling scheme is essential for accurate simulation, particularly for quasi-shear wave propagation.

Acoustic Wave Propagation Theory

Following the framework established by Vashishth and Gupta [4, 11], wave propagation in porous piezoelectric media is governed by a coupled system combining Biot's poroelasticity theory with piezoelectric constitutive relations. The governing equations consist of:

Biot's equations of motion describe the mechanical motion of the coupled solid skeleton and pore fluid:

$$\begin{aligned} \sigma_{ij,j} &= \rho_{ij}^{11}\ddot{u}_j + \rho_{ij}^{12}\ddot{u}_j^* + b_{ij}(\dot{u}_j - \dot{u}_j^*) \\ \sigma_{,i}^* &= \rho_{ij}^{12}\ddot{u}_j + \rho_{ij}^{22}\ddot{u}_j^* - b_{ij}(\dot{u}_j - \dot{u}_j^*) \end{aligned} \tag{1}$$

where σ_{ij} and σ^* are stress components for solid and fluid phases, u_i and u_i^* denote the displacement vectors, ρ_{ij}^{11}, ρ_{ij}^{12}, and ρ_{ij}^{22} are dynamic density coefficients accounting for inertial coupling, and b_{ij} represents the dissipation function related to fluid viscosity and permeability.

Piezoelectric constitutive equations relate the mechanical and electrical fields on the basis of Biot's theory:

$$\begin{aligned} \sigma_{ij} &= c_{ijkl}u_{k,l} + m_{ij}u_{k,k}^* - e_{kij}E_k \\ \sigma^* &= m_{ij}u_{i,j} + Ru_{i,i}^* \\ D_i &= e_{ikl}u_{k,l} + \xi_{ij}E_j \end{aligned} \tag{2}$$

DOI 10.5162/Ultrasonic2025/A5-a1

where c_{ijkl} are elastic stiffness coefficients, m_{ij} and R represent coupling parameters between solid and fluid phases, e_{ikl} are piezoelectric constants, ξ_{ij} are dielectric permittivity components, D_i is electric displacement, and E_i is the electric field.

Quasi-static approximation and Gauss's law assume the magnetic field is negligible, allowing the electric field to be expressed as the negative gradient of electric potential. With zero free charge density inside the medium, the electric field equations are:

$$\begin{aligned} E_i &= -\phi_{,i} \\ D_{i,i} &= \rho_e = 0 \end{aligned} \tag{3}$$

where ϕ is the electric potential and ρ_e is the free charge density. Equations (1)–(3) together constitute the complete system of governing equations.

For plane harmonic wave propagation, we seek solutions of the form:

$$(u_i, u_i^*, \phi) = (B_i, F_i, G) \exp\left[i\omega\left(\frac{n_i x_i}{v} - t\right)\right] \tag{4}$$

where ω is angular frequency, v is phase velocity, x_i denote spatial coordinates, and n_i are direction cosines of the propagation vector. Substituting the plane wave solution (4) into the governing equations (1)–(3) yields an algebraic eigenvalue problem, leading to the Christoffel equation:

$$|\mathbf{M}_{7\times7}| = 0 \tag{5}$$

This equation predicts the existence of four propagating wave modes in the medium. The analytical phase and group velocities obtained by solving Eq. (5) serve as benchmark solutions for validating the numerical FDTD scheme presented in the next section.

Numerical Simulation Framework

To simulate full wavefield propagation in porous piezoelectric media, we develop a high-order staggered-grid FDTD method that rigorously handles electromechanical coupling. We focus on a transversely isotropic medium in the 2D x_1-x_3 plane.

Beyond the mechanical equations (Eqs. (1)–(2)), the electrical field is governed by the Poisson equation derived from Gauss's law $\nabla \cdot \mathbf{D} = 0$:

$$\begin{aligned} \xi_{11}\frac{\partial^2\dot{\phi}}{\partial x^2} + \xi_{33}\frac{\partial^2\dot{\phi}}{\partial z^2} = \frac{\partial}{\partial x}\left[e_{15}\left(\frac{\partial v_x}{\partial z} + \frac{\partial v_z}{\partial x}\right)\right] \\ + \frac{\partial}{\partial z}\left[e_{31}\frac{\partial v_x}{\partial x} + e_{33}\frac{\partial v_z}{\partial z}\right] \end{aligned} \tag{6}$$

where $\dot{\phi}$ is the time derivative of electric potential. The right-hand side couples the mechanical velocity field to the electric potential. Solving this equation

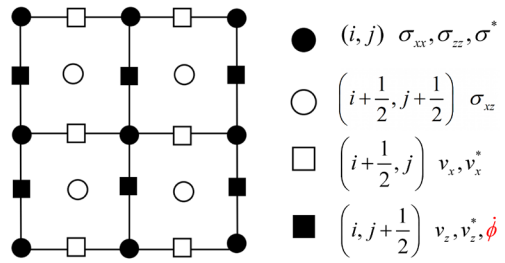

Fig. 1: Schematic of the electro-mechanical coupled staggered grid.

at every time step captures the complete dynamic electromechanical interaction. This rigorous approach differs fundamentally from simplified schemes that assume $\partial D_i/\partial t = 0$, which effectively decouples the system and introduces artificial stiffening effects [9, 10].

To implement this rigorous scheme, we design an electro-mechanical coupled staggered grid. Our key innovation is the strategic co-location of the electric potential rate $\dot{\phi}$ with the vertical velocity v_z at grid position $(i, j+\frac{1}{2})$, as shown in Fig. 1. This arrangement ensures that all spatial derivatives in both the stress-update equations (Eq. (2)) and the Poisson equation (Eq. (6)) can be computed using the same high-order stencils, preserving coupling physics with high-order accuracy and numerical stability.

Based on this grid arrangement, the time-marching algorithm proceeds in three stages at each time step.

Stage 1: Velocity Update. Velocities are updated from stress gradients using Eq. (1). For the horizontal velocity of the solid skeleton:

$$\begin{aligned} v_{x(i+1/2,j)}^{(n+1/2)} = v_{x(i+1/2,j)}^{(n-1/2)} + \Delta t\Big[\gamma_{11}\Big(D_x\sigma_{xx(i+1/2,j)}^{(n)} \\ + D_z\sigma_{xz(i+1/2,j)}^{(n)}\Big) + \gamma_{12}D_x\sigma_{(i+1/2,j)}^{*(n)} \\ + b(\gamma_{12}-\gamma_{11})\left(v_{x(i+1/2,j)}^{(n-1/2)} - v_{x(i+1/2,j)}^{*(n-1/2)}\right)\Big] \end{aligned} \tag{7}$$

where D_x and D_z denote spatial difference operators. Similar expressions apply to other velocity components. This stage follows the standard Biot poroelastic formulation without piezoelectric terms.

Stage 2: Electric Potential Solution. The Poisson equation is solved for $\dot{\phi}$ using the updated velocity

DOI 10.5162/Ultrasonic2025/A5-a1

Tab. 1: Material parameters for PZT-2 porous piezoelectric medium.

Parameter	Value	Parameter	Value
ρ_{11} (kg/m^3)	5082	c_{11} (GPa)	148.0
ρ_{12} (kg/m^3)	-1155	c_{13} (GPa)	74.2
ρ_{22} (kg/m^3)	4928	c_{33} (GPa)	131.0
e_{31} (C/m^2)	-2.324	c_{44} (GPa)	25.3
e_{33} (C/m^2)	10.99	R (GPa)	20.0
e_{15} (C/m^2)	9.3	m_{11} (GPa)	8.8
ξ_{11} (nF/m)	3.984	m_{33} (GPa)	5.2
ξ_{33} (nF/m)	2.081		

field:

$$\begin{aligned}\xi_{11}D_x^2\dot{\phi}^{(n+1/2)}_{(i,j+1/2)} + \xi_{33}D_z^2\dot{\phi}^{(n+1/2)}_{(i,j+1/2)} \\ = D_x\left[e_{15}\left(D_z v_x + D_x v_z\right)\right]^{(n+1/2)}_{(i,j+1/2)} \\ + D_z\left[e_{31}D_x v_x + e_{33}D_z v_z\right]^{(n+1/2)}_{(i,j+1/2)}\end{aligned} \tag{8}$$

The grid arrangement ensures that the source term velocities, after undergoing second-order differentiation, are naturally located at $(i, j+1/2)$, coinciding with the center position of the second-order derivatives on the left-hand side. The sparse coefficient matrix is pre-computed once, and the linear system is solved directly at each time step.

Stage 3: Stress Update. After computing the electric potential rate $\dot{\phi}$, stresses are updated from velocity and electric potential gradients using Eq. (2). For σ_{xx}:

$$\begin{aligned}\sigma^{(n+1)}_{xx(i,j)} = \sigma^{(n)}_{xx(i,j)} \\ + \Delta t\Bigg[c_{11}D_x V^{(n+1/2)}_{x(i,j)} + c_{13}D_z V^{(n+1/2)}_{z(i,j)} \\ + m_{11}\left(D_x v^{*(n+1/2)}_{x(i,j)} + D_z v^{*(n+1/2)}_{z(i,j)}\right) \\ + e_{31}D_z\dot{\phi}^{(n+1/2)}_{(i,j)}\Bigg]\end{aligned} \tag{9}$$

The term $e_{31}D_z\dot{\phi}$ represents the piezoelectric contribution. Similar expressions apply to other stress components.

Results and Validation

To validate the proposed FDTD framework and demonstrate the necessity of rigorous electromechanical coupling, we perform theoretical calculations and numerical simulations for wave propagation in transversely isotropic porous piezoelectric media. We select PZT-2 type porous piezoelectric ceramic as the representative material, with parameters listed in Tab. 1.

We first establish the analytical benchmark by solving the Christoffel equation (Eq. (5)) to obtain velocities for all wave modes as functions of propagation angle θ. As shown in Fig. 2, the theory predicts four distinct wave modes: the fast quasi-longitudinal wave (qP1), quasi-shear wave (qSV), and horizontally polarized shear wave (SH) characteristic of anisotropic elastic media, plus the slow quasi-longitudinal wave (qP2) arising from solid-fluid coupling in the porous microstructure. For transversely isotropic media with 6mm symmetry, the 7×7 Christoffel system decouples into a 2×2 system governing the SH wave (velocity independent of piezoelectric coupling) and a 5×5 system governing the three in-plane coupled modes (qP1, qSV, qP2) where electromechanical effects are significant [11]. The phase and group velocity polar plots (Fig. 2a,b) exhibit strong anisotropic characteristics reflecting material symmetry. These analytical solutions serve as rigorous benchmarks for numerical validation.

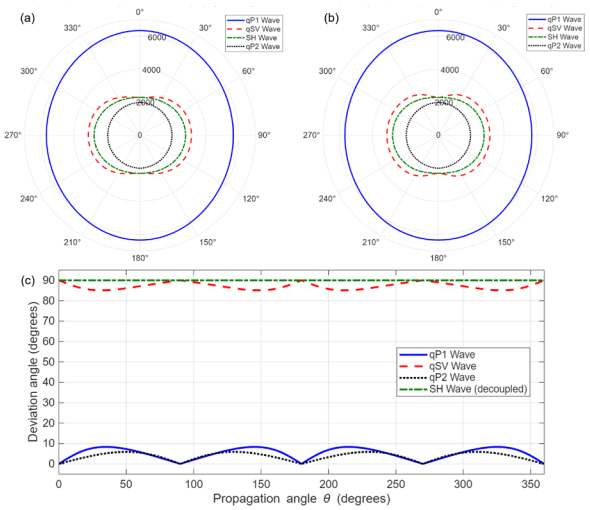

Fig. 2: Analytical solutions for PZT-2 porous piezoelectric medium: (a) Phase velocity polar plot, (b) Group velocity polar plot, (c) Skewing angle as a function of propagation angle.

The numerical FDTD simulations are performed on a 10 mm $\times$ 10 mm computational domain with spatial grid size $\Delta x = \Delta z = 25$ μm and time step $\Delta t = 2\times10^{-9}$ s. The spatial discretization employs eighth-order accuracy while time integration maintains second-order accuracy. An impulse source with center frequency $f_0 = 6$ MHz is applied at the domain center. Dirichlet boundary conditions are enforced at all boundaries.

Fig. 3 presents snapshots of multiple physical fields computed by the rigorous FDTD approach at $0.7\,\mu$s, demonstrating the comprehensive capability of the numerical framework. Clear concentric wave fronts corresponding to different modes are visible: the out-

DOI 10.5162/Ultrasonic2025/A5-a1

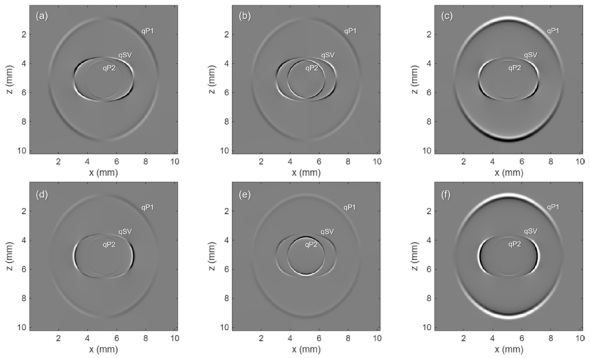

Fig. 3: Snapshots of multiple physical fields from FDTD simulations at $0.7\,\mu s$: (a) Horizontal velocity v_x of solid skeleton, (b) Horizontal velocity v_x^* of pore fluid, (c) Normal stress σ_{zz}, (d) Shear stress σ_{xz}, (e) Pore pressure σ^*, (f) Electric potential ϕ.

ermost front represents the fast qP1 wave, followed by qSV, with the slower qP2 wave in the interior. Note that the SH wave, which vibrates out of plane, cannot be captured by this two-dimensional implementation. The numerical wave speeds extracted from these wave fronts show excellent agreement with the analytical solutions in Fig. 2, confirming the accuracy of the staggered-grid FDTD method.

Having validated the numerical framework against analytical solutions, we now investigate the fundamental importance of rigorous electromechanical coupling treatment. Two approaches are compared: the simplified approach assumes $\partial D_i/\partial t = 0$, effectively decoupling the system; the rigorous approach solves the full Poisson equation (Eq. (6)) at each time step, maintaining complete dynamic coupling.

Fig. 4 presents a direct comparison between these two approaches alongside theoretical predictions. The rigorous method (center) faithfully reproduces all theoretical wave characteristics, with wave front positions matching the analytical benchmarks. Conversely, the simplified treatment (left) produces visible deviations in the wavefield structure, with the qSV wave showing the most pronounced discrepancies while qP1 and qP2 modes remain relatively unaffected.

The underlying physical mechanism stems from the constraint imposed by $\partial D/\partial t = 0$, which prevents the electric field from dynamically responding to time-varying mechanical strain. This artificially enhances the effective elastic stiffness in certain crystallographic directions, distorting wave velocities and disrupting the intrinsic anisotropic symmetry. The rigorous Poisson equation treatment, by contrast, allows the electric potential to evolve naturally in response to the instantaneous strain state, preserving both Gauss's law and correct electromechanical coupling physics.

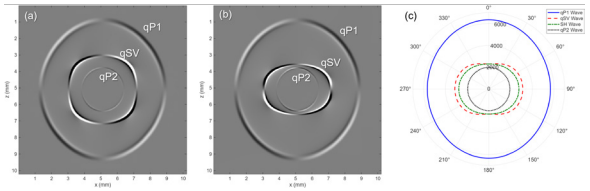

Fig. 4: Comparison of electromechanical coupling schemes: (a) Simplified approach with $\partial D/\partial t = 0$, (b) Rigorous Poisson equation approach, (c) Analytical velocity distribution from Christoffel equation.

The superior performance of the rigorous approach is fundamentally enabled by the proposed electromechanical coupled staggered grid design, ensuring numerical consistency and physical coupling accuracy.

Conclusion

This work presents an FDTD framework based on an electro-mechanical coupled staggered grid for simulating wave propagation in porous piezoelectric media. By rigorously solving the complete Poisson equation at each time step, the method accurately captures all wave modes and achieves excellent agreement with analytical solutions derived from the Christoffel equation. Compared to traditional simplified coupling schemes, the proposed method accurately simulates quasi-shear wave propagation while avoiding noticeable velocity deviations and wavefield distortions. The framework provides a robust numerical tool for investigating electromechanical wave phenomena in anisotropic porous piezoelectric materials, with applications in transducer design and piezoelectric tissue characterization.

Acknowledgment

This work was supported by the National Natural Science Foundation of China (NSFC) under Grant Nos. 42127807, 12274432, and 52227901.

References

[1] E. Mercadelli, A. Sanson, and C. Galassi. "Porous piezoelectric ceramics". In: *Piezoelectric ceramics* (2010), pp. 111–128.

[2] M. A. Biot. "Theory of Propagation of Elastic Waves in a Fluid-Saturated Porous Solid. I. Low-Frequency Range". In: *The Journal of the Acoustical Society of America* 28.2 (1956), pp. 168–178.

[3] M. A. Biot. "Theory of propagation of elastic waves in a fluid-saturated porous solid. II. Higher frequency range". In: *The Journal of the acoustical Society of america* 28.2 (1956), pp. 179–191.

[4] A. K. Vashishth and V. Gupta. "Wave propagation in transversely isotropic porous piezoelectric materials". In: *International Journal of Solids and Structures* 46.20 (2009), pp. 3620–3632.

[5] M. Sharma. "Piezoelectric effect on the velocities of waves in an anisotropic piezo-poroelastic medium". In: *Proceedings of the Royal Society A: Mathematical, Physical and Engineering Sciences* 466.2119 (2010), pp. 1977–1992.

[6] E. Filoux et al. "Modeling of piezoelectric transducers with combined pseudospectral and finite-difference methods". In: *The Journal of the Acoustical Society of America* 123.6 (2008), pp. 4165–4173.

[7] S. Rahman, H. Langtangen, and C. Barnes. "A finite element method for modelling electromechanical wave propagation in anisotropic piezoelectric media". In: *arXiv preprint physics/0510175* (2005).

[8] L. Liu, X.-M. Zhang, and X.-M. Wang. "Theoretical analysis and numerical simulation of acoustic waves in gas hydrate-bearing sediments". In: *Chinese Physics B* 30.2 (2021), p. 024301.

[9] F. Chagla and P. M. Smith. "Finite difference time domain methods for piezoelectric crystals". In: *IEEE transactions on ultrasonics, ferroelectrics, and frequency control* 53.10 (2006), pp. 1895–1901.

[10] Y.-y. Zhao et al. "Finite difference time domain analysis of two-dimensional piezoelectric phononic crystals". In: (2012), pp. 1–4. DOI: 10.1109/SPAWDA.2012.6464021.

[11] A. K. Vashishth and V. Gupta. "Decoupling of plane waves in porous piezoelectric materials". In: *Proceedings of the Royal Society A: Mathematical, Physical and Engineering Sciences* 470.2169 (2014), p. 20140172.